Redox Biology 81 (2025) 103524

Contents lists available at ScienceDirect

Redox Biology

journal homepage: www.elsevier.com/locate/redox

Quantitative analysis of the proteome and protein oxidative modifications in primary human coronary artery endothelial cells and associated extracellular matrix

Shuqi Xu [a,b], Christine Y. Chuang [a], Clare L. Hawkins [a], Per Hägglund [a,**,1], Michael J. Davies [a,*,1]

[a] Department of Biomedical Sciences, Panum Institute, University of Copenhagen, Denmark
[b] Department of Cardiovascular Medicine, The Affiliated Yongchuan Hospital of Chongqing Medical University, Chongqing, China

ARTICLE INFO

Keywords:
Endothelial cells
Proteomics
Extracellular matrix
Oxidative modifications
Post-translational modification
Protein oxidation
Protein hydroxylation
Protein nitration

ABSTRACT

Vascular endothelial cells (ECs) play a key role in physiology by controlling arterial contraction and relaxation, and molecular transport. EC dysfunction is associated with multiple pathologies. Here, we characterize the cellular and extracellular matrix (ECM) proteomes of primary human coronary artery ECs, from multiple donors, and oxidation/nitration products formed on these during cell culture, using liquid chromatography-mass spectrometry. In total ~9900 proteins were identified in cells from 3 donors, with ~7000 proteins per donor. Of these ~5300 were consistently identified, indicating some heterogeneity across the donors, with age a possible cause. Multiple endogenous oxidation products were detected on both ECM and cellular proteins (and particularly endoplasmic reticulum species). In contrast, nitration was mostly detected on cell proteins and particularly cytoskeletal proteins, consistent with intracellular generation of nitrating agents, possibly from endothelial nitric oxide synthase (eNOS) or peroxidase enzymes. The modifications are ascribed to both physiological enzymatic activity (hydroxylation at proline/lysine; predominantly on ECM proteins and especially collagens) and the formation of reactive species (oxidation at tryptophan/tyrosine/histidine; nitration at tryptophan/tyrosine). The identified sites are present on a limited number of peptides (104 oxidized; 23 nitrated) from a modest number of proteins. A small number of proteins were detected with multiple modifications, consistent with these being selective and specific targets. Several nitrated peptides were consistently detected across all donors, and also in human smooth muscle cells suggesting that these are major targets in the vascular proteome. These data provide a 'background' proteome dataset for studies of endothelial dysfunction in disease.

1. Introduction

Endothelial cells (ECs) form a monolayer that lines the lumen of blood vessels, with this commonly referred to as the vascular endothelium [1,2]. ECs are polarized, with their luminal plasma membrane being decorated with extracellular matrix (ECM) molecules (the

Abbreviations: ACN, acetonitrile; BCA, bicinchoninic acid assay; DDA-PASEF, data-dependent acquisition with parallel acquisition-serial fragmentation; DIA-PASEF, data-independent acquisition with parallel acquisition-serial fragmentation; DTT, dithiothreitol; EC, endothelial cell; ECM, extracellular matrix; FA, formic acid; FASP, filter-aided sample preparation; FDR, false discovery rate; HCAEC, human coronary artery endothelial cells; HCASMC, human coronary artery smooth muscle cell; LC-MS, liquid chromatography-mass spectrometry; LFQ, label-free quantification; ONOOH/$ONOO^-$, the physiological mixture of peroxynitrous acid and its conjugate anion peroxynitrite; PB, 100 mM phosphate buffer, pH 7.4; PBS, phosphate-buffered saline; PCA, principal component analysis; PTMs, post-translational modifications; SDS, sodium dodecyl sulfate; SEC, size exclusion chromatography; STAGE, stop-and-go-extraction; TFA, trifluoroacetic acid; TIMS, trapped ion mobility spectrometry; TOF, time-of-flight.

* Corresponding author. Department of Biomedical Sciences, Panum Institute, University of Copenhagen, Building 12.6.30, Blegdamsvej 3, 2200, Copenhagen, Denmark.

** Corresponding author. Department of Biomedical Sciences, Panum Institute, University of Copenhagen, Building 12.6.30, Blegdamsvej 3, 2200, Copenhagen, Denmark.

E-mail addresses: pmh@sund.ku.dk (P. Hägglund), davies@sund.ku.dk (M.J. Davies).

[1] Joint senior and corresponding authors.

https://doi.org/10.1016/j.redox.2025.103524
Received 5 December 2024; Received in revised form 28 January 2025; Accepted 30 January 2025
Available online 6 February 2025

glycocalyx), while their basolateral surface is separated from surrounding tissues by a basement membrane of ECM molecules encoded by the ECs [3]. The endothelial barrier arising from this EC monolayer and associated ECM, has a high selectivity and regulates the movement of molecules, cells (e.g. platelets and white blood cells) and fluids into and out of the artery wall from the bloodstream, with this being dependent on the microenvironment and arterial type [4,5]. ECs play a key role in modulating vascular relaxation, particularly via the production of nitric oxide ($NO^{\bullet}$) generated by endothelial nitric oxide synthase (eNOS), and constriction, blood fluidity, platelet adhesion and aggregation, leukocyte activation, adhesion and transmigration [4]. The ECs maintain a delicate balance between coagulation and fibrinolysis, and are involved in regulating immune responses, inflammation, and angiogenesis [6], with their luminal surface having antithrombotic and anticoagulant activities, achieved (in part) by the glycocalyx, and the regulated secretion of antiplatelet agents including prostacyclin and $NO^{\bullet}$ [6].

Lifestyle factors and disease, including smoking and physical inactivity, and hypertension and diabetes, can lead to EC dysfunction and a loss of integrity and properties of the monolayer and associated ECM [7], with this resulting in a shift from homeostasis towards a pro-inflammatory response. This is accompanied by diminished vasodilation and increased proliferative and pro-thrombotic properties [8]. Endothelial dysfunction has been associated with angiogenesis in cancer, vascular leakage, stroke and atherosclerosis (reviewed [9]).

The critical role of ECs in the pathogenesis of atherosclerosis, the major underlying cause of most cardiovascular disease, is well-established [10], with endothelial dysfunction being a hallmark of the disease [11]. Atherosclerosis is characterized by impaired vasodilation, increased permeability of the endothelial barrier, and pro-inflammatory activation of ECs induced by various risk factors including hyperlipidemia, hypertension, diabetes and smoking [12]. These risk factors are associated with oxidative stress and inflammation, which promote the recruitment of neutrophils, monocytes and lymphocytes to the sub-endothelial space, where the monocytes differentiate into macrophages, which take up modified (aggregated, oxidized, glycated or otherwise modified) low-density lipoproteins in an unregulated manner to form lipid-laden (foam) cells [12]. Accumulation of lipids, foam cells, and subsequent cell death results in plaque formation and disease progression. ECs also contribute to plaque development by regulating the recruitment, adhesion and migration of immune cells, and by secreting cytokines and growth factors that promote the proliferation, migration and de-differentiation of smooth muscle cells (SMCs). These events are believed to be associated with, and perhaps driven by, alterations to the protein complement (proteome) of ECs [13–16].

Remodeling of the arterial ECM occurs during the course of atherosclerosis, and alterations to the ECM impact on the progression of atherosclerosis [17–22]. Thus, the arterial ECM not only serves as a vital structural component of plaques, but also influences the behavior of both ECs and SMCs. Understanding the pathogenesis of atherosclerosis therefore requires knowledge of the proteome of each of the major cell types present in the artery wall, their surrounding ECM and how these alter during disease development. We have recently reported on the proteome of human coronary artery smooth muscle cells (HCASMC), and post-translational modifications (PTMs) detected on both the cell and ECM proteome [23]. The current study provides comparable data for human coronary artery ECs (HCAEC) isolated from multiple donors. Together these data provide a foundation for unraveling the vascular proteome dynamics that may occur during the development of atherosclerosis, and provide avenues for exploring innovative therapeutic interventions, as many drug targets are proteins.

2. Materials and methods

2.1. Materials

Chemicals were obtained from Sigma-Aldrich-Merck (Søborg, Denmark) unless stated otherwise. Mass spectrometry-grade water, acetonitrile (ACN), DMSO and formic acid (FA) were obtained from VWR (Søborg, Denmark). Trypsin (sequencing grade, modified) was purchased from Promega (Finnboda, Sweden). Primary HCAEC were obtained from 3 donors (#2366, 60 year old Caucasian male; #3003, 38 year old Caucasian male; #3118, 31 year old Caucasian male), together with corresponding growth media, from Cell Applications (San Diego, CA). No further data are available on these donors.

2.2. Cell culture

Cells were cultured up to passage 5 in a humidified incubator at 37 °C with 5 % CO_2 and 20 % O_2 using commercial HCAEC growth media (Cell Applications). The initial seeding density was 10^6 cells in 25 mL of medium in 175 cm^2 flasks. The growth medium was replaced three times per week, and the cells were maintained for 7 days to allow the cells to generate a native ECM. Three biological replicates were established for each cell donor.

2.3. Protein extraction

After 7 days in culture, the cells and associated ECM were solubilized by overnight incubation at 4 °C with gentle rocking, using 8 M urea in Tris-HCl (0.1 M, pH 8.0), supplemented with a protease inhibitor cocktail (Sigma-Aldrich) at a dilution of 1:100. This cocktail includes EDTA, which will inhibit adventitious metal ion mediated reactions. The samples were then collected in 15 mL tubes and centrifuged (20 min, 220 g) to precipitate insoluble material. The resulting supernatants were then transferred and concentrated using Vivaspin® 6 centrifugal filtration units, using a 10 kDa cutoff filter (12,000 g, 4 °C), and washed three times with phosphate-buffered saline (PBS). The protein concentration in the samples was determined using the bicinchoninic acid (BCA) assay.

2.4. Size exclusion chromatography (SEC)

For some cell samples, SEC was performed prior to liquid chromatography-mass spectrometry (LC-MS/MS) analysis with the protein preparations subjected to gel filtration at 21 °C using a using a Superose 6 Increase 10/300 GL column (GE Healthcare) on an Äkta FPLC system (GE Healthcare) equilibrated with 100 mM phosphate buffer (pH 7.4, PB), containing 0.1 % v/v SDS, at a flow of 0.5 mL min^{-1}. The absorbance of the eluent was monitored at 280 nm, with 1 mL fractions collected for subsequent analysis.

2.5. Filter-aided sample preparation (FASP) for LC-MS/MS

A volume of 145 μL of sample (~15 μg protein) was combined with 200 μL of 8 M urea in 0.1 M Tris-HCl, pH 8.5, and centrifuged (14,000 g, 20 min, 21 °C) in spin filters (Vivacon®500, 10 kDa molecular mass cut off). Subsequently, 360 μL of 8 M urea in 0.1 M Tris-HCl, pH 8.5, and 40 μL of 500 mM dithiothreitol (DTT) to reduce disulfide bonds, were added to the concentrate and incubated for 30 min, followed by further centrifugation (as above). The resulting concentrate was diluted using 360 μL of 8 M urea in 0.1 M Tris-HCl, pH 8.5, and treated with 40 μL of 500 mM iodoacetamide to alkylate free thiols, with the samples incubated in the dark for 30 min. The samples were then subsequently re-centrifuged as described above, with the concentrate diluted with 400 μL of 8 M urea in 0.1 M Tris-HCl, pH 8.0, and concentrated again through centrifugation, with this step repeated twice. Subsequently, 400 μL of 1.6 M urea in 0.1 M Tris-HCl, pH 8.0, was added and the samples subjected to centrifugation, with this repeated twice. The

reduced and alkylated proteins in the concentrated samples were then digested using sequencing grade trypsin (0.2 μg trypsin in 1.6 M urea in 0.1 M Tris-HCl, pH 8.0) at 21 °C overnight. The peptides in the digests were then collected by centrifugation of the samples through a 10 kDa filter with the filter subsequently rinsed with 50 μL of 0.5 M NaCl and re-centrifuged to recover any residual peptides. The combined flow-through was then used for subsequent steps.

2.6. Sample pre-treatment by stop-and-go-extraction tips (StageTips)

In-house generated StageTips were constructed by placing two C18 filter discs within a 200 μL pipette tip, and used to concentrate and purify the tryptic peptides [24]. The discs were activated by sequential addition, and centrifugation at 1200 g and 21 °C, of 50 μL methanol, 50 μL 80 % acetonitrile (ACN)/0.1 % trifluoroacetic acid (TFA) in water, and finally 50 μL 0.1 % TFA in water. Tryptic peptides, acidified with 10 μL TFA (from a 10 % stock v/v solution), were subsequently loaded onto the tip. Following two washes with 50 μL 0.1 % TFA in water, the peptides were eluted with 50 μL 80 % ACN/0.1 % TFA in water. The eluent was then collected and vacuum-dried at 21 °C.

2.7. Mass spectrometric (MS) analyses

Samples were reconstituted in 50 μL 0.1 % FA in water and analyzed on a Bruker Tims-ToF PRO mass spectrometer (Bruker Daltonics, Bremen, Germany) in the positive ion mode with an online Captivespray ion source connected to a Dionex Ultimate 3000RS nano chromatography system (Thermo Fisher Scientific). Peptides were separated on an Aurora column (C18, 1.6 μm, 25 cm, 75 μm ID; IonOpticks, Fitzroy, Australia) at 60 °C with a solvent gradient using 0.1 % FA in water (Solvent A) and 99.9 % ACN/0.1 % FA in water (Solvent B), at a flow rate of 400 nL min^{-1}. The amount of Solvent B was increased linearly from 2 % to 5 % over 4 min, 5–25 % over 90 min, 25–35 % over 10 min, and 35–85 % over 10 min, before re-equilibration with the starting composition and injection of the next sample. The spectrometer was operated in either a data-dependent acquisition with parallel acquisition-serial fragmentation (DDA-PASEF [25]) mode, or a data-independent acquisition PASEF mode (DIA-PASEF [26]), with 1.1 s cycle time, and a TIMS ramp time of 100 ms. The precursor and fragment scan ranges were set to 350–1700 and 100–1800 *m/z*, respectively.

For protein identification and quantification using DDA-PASEF, the data were searched against the human UniProt reference proteome (UP000005640, downloaded on 2021-11-11), including common contaminants, using Fragpipe version 19.0 with MSFragger version 3.7, IonQuant 1.8.10 and Philosopher version 4.8.1 [27]. The following settings were used: trypsin with 2 missed cleavages; precursor mass tolerance (20 ppm); fragment ion mass tolerance (20 ppm). The modifications employed were: carbamidomethylation of Cys (+57.0215 Da; fixed), N-terminal acetylation (+42.0106 Da; variable) and oxidation of Met (+15.9949 Da; variable). The precursor and peptide-level false discovery rate (FDR) was set to 1 % with label-free quantification (LFQ) without match-between runs. PTM specific searches of DDA-PASEF data were performed as described above, but with Fragpipe 20.0 (including MSFragger version 3.8, IonQuant 1.9.8 and Philosopher version 5.0.0) and oxidation of Met/Tyr/Trp/His/Lys/Pro (+15.9949 Da) and nitration of Tyr/Trp (+44.9851 Da) as additional variable modifications.

The DIA-PASEF database searches were performed using DIA-NN (version 1.8) [27] with a spectral library generated *in silico* from the human UniProt reference proteome (UP000005640) using the following parameters: trypsin with 1 missed cleavage; cysteine carbamidomethylation (fixed modification), methionine oxidation and *N*-terminal acetylation (variable modifications); peptide charge: 2–4; peptide length: 7–25); precursor FDR: 1 %. The mass spectrometry proteomics data have been deposited to the ProteomeXchange Consortium via the PRIDE partner repository with the dataset identifier PXD056929.

Data from PXD037861 [28] was analyzed using Fragpipe as described above. Data from PXD006675 [29] was analyzed using MaxQuant 2.0.2.0 (FDR: 1 %; 20 ppm precursor and fragment ion mass tolerance; maximum 2 missed cleavage, with trypsin as enzyme). The modifications employed were: carbamidomethylation of Cys (+57.0215 Da; fixed), N-terminal acetylation (+42.0106 Da; variable), oxidation of Met (+15.9949 Da; variable) nitration of Tyr/Trp (+44.9851 Da; variable).

2.8. Data analysis, visualization, statistical analyses and errors

For protein identification and quantification, only proteins identified in all 3 independent experiments for each condition, were used for analysis. Volcano plots were generated using the R package limma (version 3.40.6) to identify differentially expressed proteins between two groups. The protein profile dataset was first log2-transformed, then the lmFit function was applied to perform multiple linear regression. Subsequently, the eBayes function was employed to compute moderated t-statistics, moderated F-statistics, and log-odds of differential expression by empirical Bayes moderation of the standard errors towards a common value. This process resulted in the determination of the statistical significance of differential proteins. The following thresholds were set for significance: P-value <0.05, FDR <0.05, and a fold change greater than 2.

In the PTM analyses, only modified peptides identified in at least 2 out of 3 biological replicates from at least one experimental group (unfractionated, CF1, CF2, CF3) were subjected to detailed analysis including evaluation of chromatographic retention times, spectral quality and correct isotopic assignments. Transcriptome data for endothelial cells were downloaded from The Human Protein Atlas (https://www.proteinatlas.org/) using the command string: cell_type_category_rna:Endothelial cells; Detected in all, Detected in many, Detected in some, Detected in single. The Matrisome dataset used for reference classification was sourced from MatrisomeDB 2.0 (MatrisomeDB: 2023 updates of the ECM protein knowledge database [30]). Data plots were generated using Hiplot (https://hiplot.org).

3. Results

3.1. Workflow

Fig. 1 provides an overview of the experimental workflow employed to examine the proteome of primary human coronary artery endothelial cells (HCAEC) and their associated ECM. The HCAEC were examined at an early and consistent passage number (five), to minimize potential differences arising from different cell ages and de-differentiation. Material from three donors (3 biological replicates from each donor; all male but of different ages, see Materials and methods) were analyzed to allow the consistency and reproducibility of identifications across the different donors to be examined. Both cellular and ECM proteins were assessed using two different data acquisition methods (DDA-PASEF and DIA-PASEF [25,26]).

3.2. Comparison of fractionation versus unfractionated analysis

Analyses were carried out on both unfractionated and SEC-fractionated samples to determine whether the latter enhanced the number (breadth) and quality of the data, with these samples examined using both data acquisition methods. Fig. 2A displays representative SEC chromatograms (optical absorption at λ 280 nm) of samples from each of the donors, with three independent biological replicates for each. These indicate a high consistency between the three chromatograms of the biological replicates obtained from each donor, confirming the reliability of the protein extraction method. However, it is also clear that there are differences between the 3 donors in the elution profiles of the proteins eluted from the SEC, with the profiles for EC3003 and EC3118 exhibiting a greater degree of similarity when compared to EC2366. As

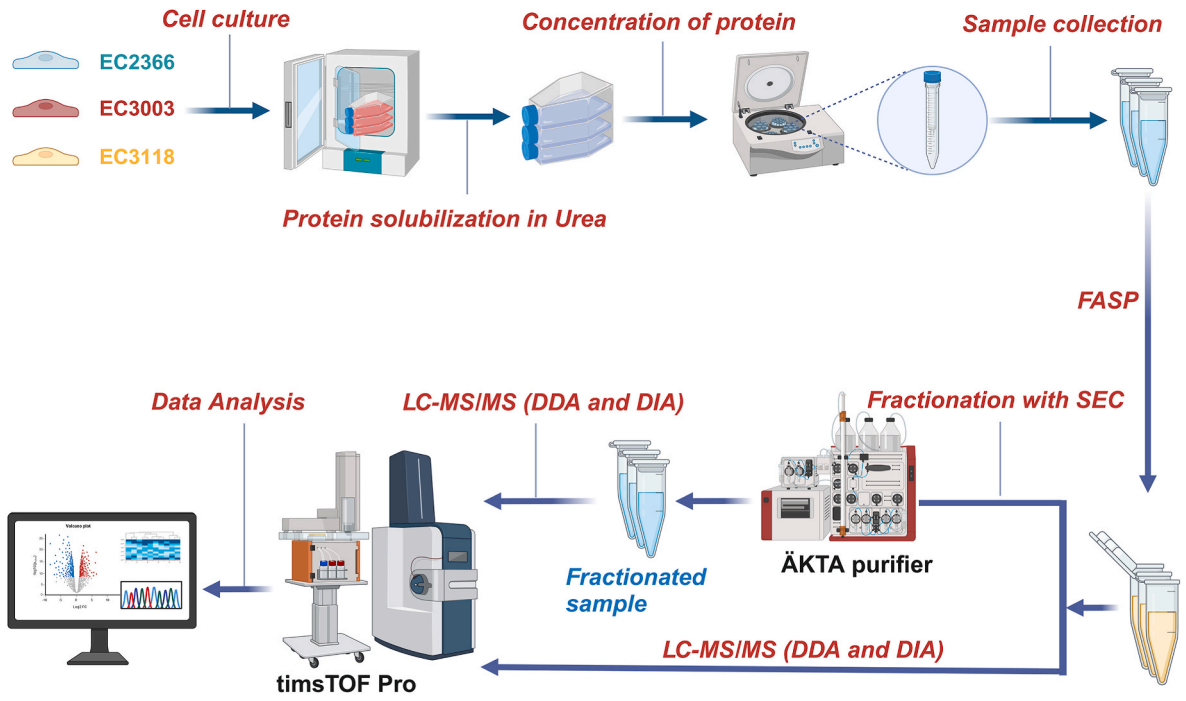

Fig. 1. Schematic representation of the experimental workflow in this study. Endothelial cells from three different donors (EC2366, EC3003, EC3118) were cultured for 7 days in flasks at passage 5 (see Materials and methods). Subsequently, the culture media was removed, and the cultures washed with PBS, before solubilization of the cellular proteins and surrounding ECM using 8 M urea at pH 8.0. The samples were then concentrated by ultrafiltration, followed by filter-assisted sample preparation (FASP) with trypsin digestion. A portion of the samples was directly analyzed by LC-MS/MS, while another portion was subjected to size exclusion chromatography (SEC) using an ÄKTA system, with the collected fractions then analyzed by LC-MS/MS.

the number of fractions collected was large, which would make LC-MS/MS analyses unrealistic (due to the large amounts of machine time required), some of the fractions were merged, as indicated in Fig. 2B. Thus, fractions A8 - A12 were combined to form CF1 (Combined Fraction 1), while A13, A14, A15, B15, and B14 were merged to form CF2, and B10 – B13 were combined to give CF3. These combined fractions were concentrated, and subsequently analyzed in the same manner as the unfractionated samples.

3.3. Comparison of data-dependent (DDA) and data-independent acquisition (DIA) methods

Fig. 2C1 presents a comparative analysis of the number of proteins detected and quantified, using these different methods, for each of the 3 donors (complete lists of identified proteins are presented in Supplementary Data File 1). In general, DIA gave higher numbers of total identifications than DDA. Within the DIA samples, the fractionated materials allowed the identification of more proteins when compared to unfractionated samples. However, in the DDA series, the opposite trend was observed, though this was less pronounced, with unfractionated samples allowing the identification of slightly more proteins than fractionated ones.

Fig. 2C1 and Fig. 2C2 provide data on the number of individual identifications and the extent of overlap between the different data analysis methods, and the unfractionated/fractionated samples, across each of the donors. In each case, large numbers of common proteins were detected across the methods. For the DDA approach, the number of common identifications between fractionated and unfractionated samples was in the range ~2600–3400.

The situation with the DIA data was somewhat different, with the number of common identifications being considerably higher than for the DDA approach (e.g. 4619 versus 2674 for EC2366) and in the range of 1.52–1.72-fold (Fig. 2C2). In this case, fractionation gave higher numbers of identifications than the unfractionated samples (e.g. 6940 vs 4257 for EC3003), though there was variation across the donors in the extent of this increase. When similar samples were compared directly using DIA versus DDA analysis methods, it was clear that DIA provided significant advantages over DDA in terms of total numbers of identifications, with more unique identifications detected with DIA than with DDA. Overall, these data indicate that DIA provides much higher numbers of identifications than DDA, and that fractionation did not provide major advantages with DDA analysis, but did with DIA, though the extent of this increase was donor dependent.

3.4. Total proteome of ECs

The total proteome for each HCAEC donor was assessed by combining the data obtained for the fractionated and unfractionated methods with that from both the DDA and DIA approaches. Only proteins present in all biological replicates from cells for a particular donor were considered, with these then considered across all 3 donors. The resulting data are presented in Fig. 2D. The protein identifications have been grouped using the gene ontology (GO) term 'Cellular Component' in Supplementary Data File 2 to facilitate searching for data from particular organelles and cellular components. In total, 7102 proteins were identified in EC2366, 7174 in EC3003, and 7815 in EC3118. When data from all three donors were assessed, 5306 proteins were consistently identified of the 9903 detected in total (sum of all the identifications; Fig. 2D), but significant numbers were also detected in only two donors (320–647 proteins) or a single subject (867–1253 proteins). These data indicated that there is a high degree of heterogeneity across the 3 donors examined, with only 68–75 % of the total proteins detected as common species for any particular donor, and ~54 % of all the identifications (5306 of 9903 total). Some of this variation is likely to arise from the challenges in detecting low abundance proteins, and limitations in the dynamic range of the mass spectrometer.

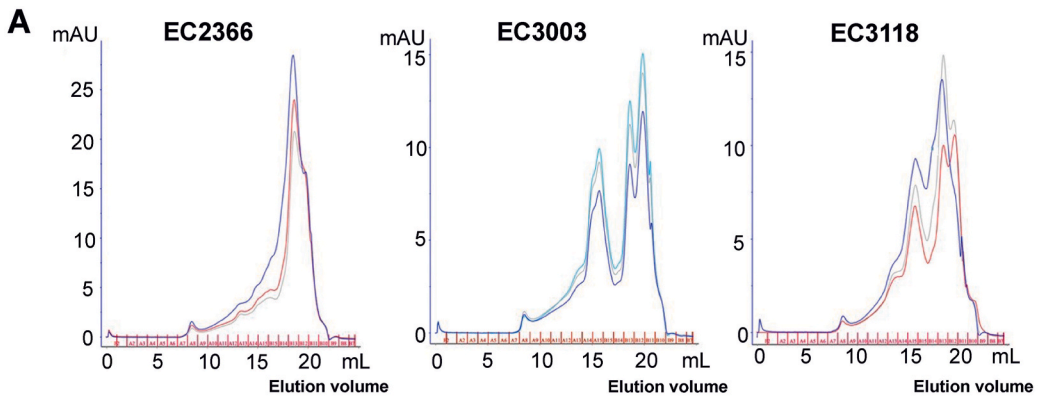

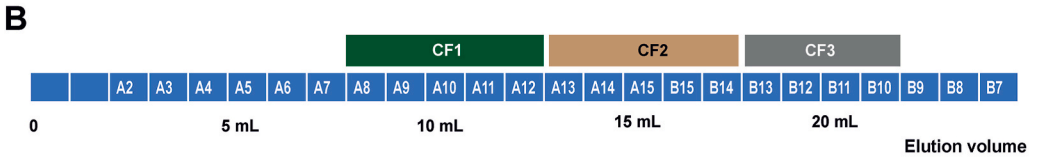

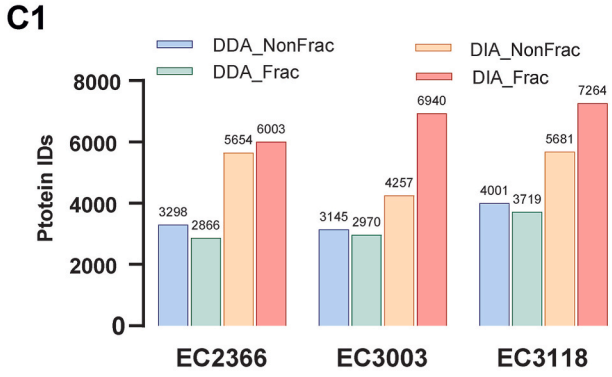

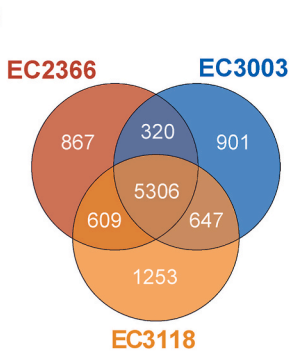

C2

Sample											
EC2366_DDA_Frac	●						●				
EC3003_DDA_Frac		●						●			
EC3118_DDA_Frac			●						●		
EC2366_DDA_NonFrac	●									●	
EC3003_DDA_NonFrac		●									●
EC3118_DDA_NonFrac			●								
EC2366_DIA_Frac				●			●				
EC3003_DIA_Frac					●			●			
EC3118_DIA_Frac						●			●		
EC2366_DIA_NonFrac				●						●	
EC3003_DIA_NonFrac					●						●
EC3118_DIA_NonFrac						●					●
Number of shared proteins	**2674**	**2650**	**3463**	**4619**	**4116**	**5259**	**2780**	**2917**	**3603**	**3213**	**2908**	**3742**

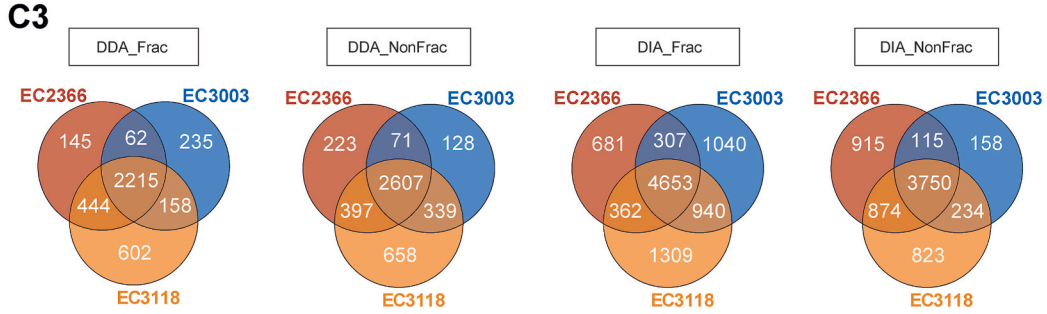

(caption on next page)

Fig. 2. Data on the proteins detected and quantified using different experimental approaches. (A) Elution profile of protein preparations (with 3 biological replicates of each) from EC2366, EC3003 and EC3118. (B) Schematic representation of the combination of fractions for the subsequent LC-MS/MS analyses. (C1) Number of protein IDs detected in different HCAEC donors using different analytical methods. DDA_NonFrac: samples processed without fractionation and analyzed by DDA-PASEF. DDA_Frac: samples processed with fractionation and analyzed by DDA-PASEF. DIA_NonFrac: samples processed without fractionation and analyzed by DIA-PASEF. DIA_Frac: samples processed with fractionation and analyzed by DIA-PASEF. (C2) The number of shared proteins identified under specified sample preprocessing methods (with or without fractionation) and MS acquisition modes (DDA or DIA). (C3) Venn diagram analysis of the proteins identified in different HCAEC donors under various sample preprocessing methods (with or without fractionation) and MS acquisition modes (DDA or DIA). (D) Venn diagram comparison of proteins detected in different HCAEC donors. The sets of each cell donor include all proteins identified through DDA-PASEF- and DIA-PASEF LC-MS/MS analyses, with and without fractionation.

3.5. Comparison of proteome and transcriptome data

The common identifications detected by all methods and all donors, as well as the total identifications were compared to previously reported EC transcriptome data to determine what percentage of the predicted protein complement was detected (Fig. 3). The vascular endothelial cells were identified based on single-cell sequencing and derived from tissues including breast, endometrium, esophagus, fallopian tube, heart muscle, liver, lung, ovary, pancreas, placenta, prostate, salivary gland, skeletal muscle, skin, testis, thymus, tongue, and vascular tissues. Of the 5306 common proteins, 4720 show commonality with the transcriptome data, with 586 proteins detected that were not present in the transcriptome. Conversely, 8787 transcripts were not detected at the protein level. For the total (9903) identifications, 7734 were also detected in the transcriptome.

3.6. Comparison of protein identification data between HCAEC donors

Principal component analysis (PCA) was performed on the proteomes detected in the biological replicates from the different donors (Fig. 4A). The first two principal components explained a cumulative variance of 88.4 %, indicating that these two dimensions effectively capture the majority of the data characteristics. The three biological replicates from each individual donor are tightly clustered, but the different donors are separated from each other. Heatmap analysis of the 3750 proteins identified across all three HCAEC donors yielded similar results (Fig. 4B). Notably, EC3003 and EC3118 exhibited a much greater degree of similarity than either of these donors when compared to EC2366, consistent with the elution profiles observed in SEC (Fig. 2A). Cluster analysis of the heat map revealed 6 groups of proteins with different abundance patterns among the three donors (Fig. 4C, with detailed analysis provided in Supplementary Data File 3). Differential expression analysis of the proteins detected from each cell donor was conducted (Fig. 4D and Supplementary Data File 4).

3.7. Identification and quantification of matrix proteins from the HCAEC donors

The majority of both the common, and total protein identifications detected across the 3 donors are of cellular origin (Fig. 5A and B; Supplementary Data File 2). This is consistent with previous studies that have reported larger numbers of cellular compared to ECM proteins, though the latter are often more abundant in terms of *quantity* in tissues (e.g. Ref. [21]). Of the common identifications (5306 proteins) detected across all donors, 5100 are described as cellular using the classifications reported in MatrisomeDB 2.0 [30], with 206 listed as ECM and ECM-associated. Of the latter, 78 categorized are core matrix (matrisome) and 128 matrisome-associated, with these accounting for ~4 % (in terms of identifications) of the total detected proteome. Of the total number of identified proteins (9903 across all 3 donors), 9501 were classified as cellular proteins and 402 as ECM and ECM-associated, with the latter comprising 145 core matrisome components, and 257 matrisome-associated. Of these 402 ECM species, 206 were common to all three donors (Fig. 5C). As representative of major ECM proteins, we analyzed the different isoforms of collagens and laminins in greater detail. Most collagen isoforms were detected across all three EC donors, except for COL6A2, which was only identified in EC3003. Similarly, COL11A2, COL12A1, and COL13A1 were detected in only one donor each (EC3118, EC3003 and EC3118 respectively). COL10A1 was identified in both EC2366 and EC3003, but not in EC3118 (Fig. 5D). Of the laminin isoforms detected, LAMA4, LAMA5, LAMB1, LAMB2, and LAMC1 were identified in all three donors, while LAMA2 was only detected in EC3118, and not in the other two donors (Fig. 5E).

3.8. Detection of oxidative post-translational modifications

The feasibility of detecting post-translational protein modifications on HCAEC proteins (both cellular and ECM) using the proteomics approaches discussed above was evaluated with a focus on the detection of oxidized and nitrated species. Such modifications can arise from both enzymatic and non-enzymatic reactions (reviewed [31]) and can both be intended site-specific enzymatic processes (e.g. hydroxylation of lysine, Lys, and proline, Pro, residues during ECM protein processing [32]), or from (presumed) unintended oxidative insults (e.g. Refs. [31,33]). Whilst many studies have focused on one or other of these events, and at specific residues (e.g. methionine, Met, or cysteine, Cys, residues), modifications can occur on a range of other residues. In the current study, database searches were performed to identify oxidation/hydroxylation at Tyr, Trp, His, Lys, Pro and Met. This resulted in detection of 4456–5019 putatively modified peptides derived from proteins from

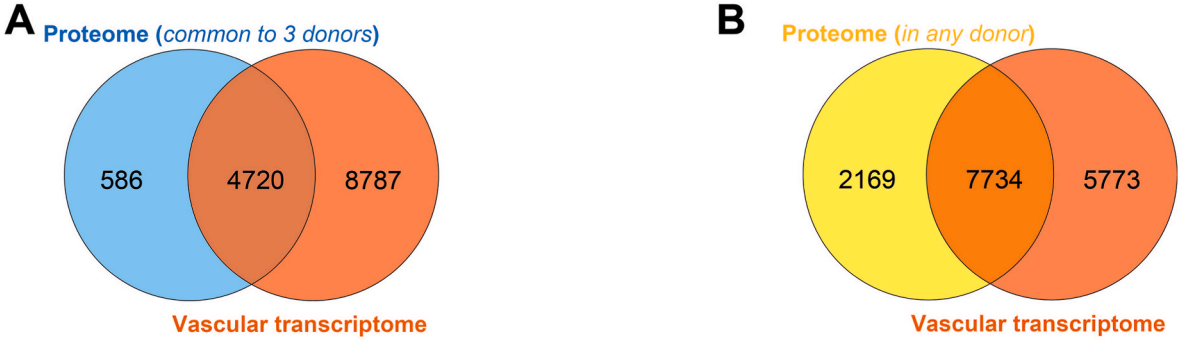

Fig. 3. Comparison of EC proteomics (this study) and reported transcriptomic data. The Venn diagrams showing overlap between the vascular endothelial transcriptome and proteins common to all three cell donors (A) or proteins detected in any cell donor (B).

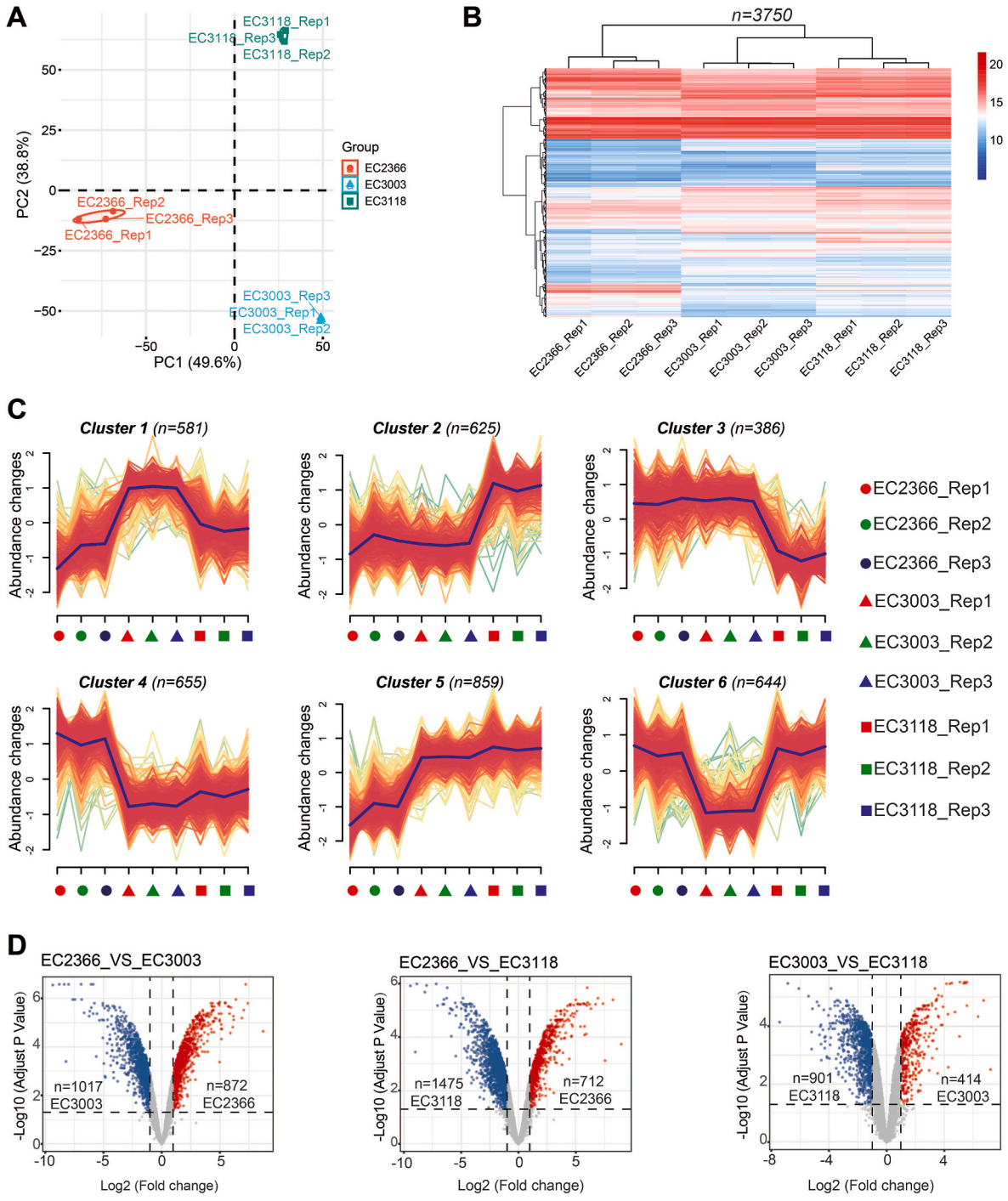

Fig. 4. Comparison of the proteome profiles of each cell donor based on samples processed without fractionation and analyzed by DIA-PASEF mass spectrometry. (A) Principal component analysis (PCA) and (B) heat map analysis plot of log2 transformed label-free quantification (LFQ) intensities of the proteins identified from EC2366, EC3003 and EC3118. Rep1, Rep2 and Rep3 represent the three biological replicates from each donor. (C) Cluster profile plot showing patterns of protein abundance changes across different cell donors. (D) Volcano plot indicating differential protein expression between pairs of the three different donors.

each of the individual cell donors (Supplementary Table 1). Of these, 1604–2148 were reproducibly detected in at least two of three biological replicates from one of the experimental conditions (e.g. unfractionated, CF1, CF2 or CF3). These searches were refined by excluding Met-containing peptides as these might be artifactually-modified during sample processing. This yielded 398–553 peptides from the cells of individual donors. Of these, 255 were identified in the samples from at least two different cell donors, indicating either sites of deliberate enzymatic oxidation, or sites particularly sensitive to unintended modification. These peptides were subjected to more detailed analysis, including evaluation of chromatographic retention times, spectral quality and correct isotopic assignments. A total of 104 peptides, covering 162 putative oxidation sites passed this evaluation, with 89, 85, and 97 of these peptides detected in EC2366, EC3003 and EC3118, respectively (Fig. 6). Among these, the most frequently assigned oxidized residue was Pro, followed by Trp, Lys, His and Tyr (Fig. 6). In a limited number of cases, the assignment of the specific oxidation site is ambiguous, due to the presence of several potential oxidation sites in close vicinity. In addition, some peptides were detected with two added oxygen atoms that might arise from di-oxidation at a single residue, or

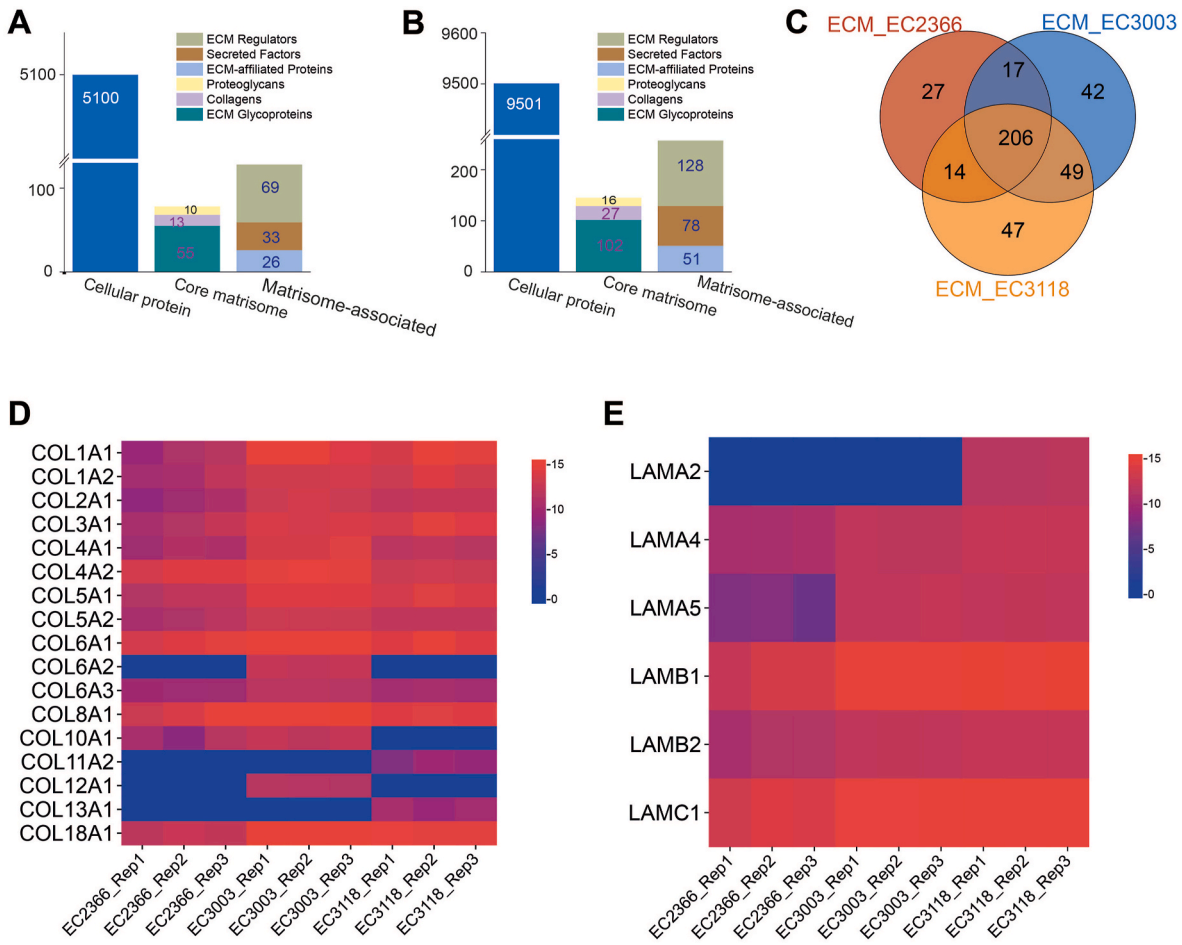

Fig. 5. Cell, ECM and ECM-associated proteins detected and quantified from the different HCAEC donors. Stack bar plot showing the number of cellular proteins, core matrisome, and matrisome-associated proteins identified in all three EC donors (A; 5306 proteins in total) or in any of the three EC donors (B; 9903 proteins in total). (C) Venn diagram comparison of ECM (core matrisome and matrisome-associated) species detected in different HCAEC donors. The data presented for each cell donor includes all proteins identified by either DDA-PASEF or DIA-PASEF LC-MS/MS from both directly assessed and fractionated samples. Isotypes of (D) collagens and (E) laminins identified and quantified across the three different HCAEC donors, based on samples processed without fractionation and analyzed by DIA-PASEF.

mono-oxidation of two different residues (Supplementary Table 2). A number of the peptides with oxidized Pro have been assigned to collagens types I, II, IV and V. Oxidation was also detected on a number of other ECM proteins, including laminin, fibronectin and vimentin (Table 1). Other proteins detected with significant levels of modifications include those derived from the endoplasmic reticulum (ER), with 10 peptides from protein disulfide-isomerases detected with oxidation primarily at Pro (Supplementary Table 2). Other ER proteins detected with oxidized residues include calnexin, calreticulin and peptidyl-prolyl *cis*-trans isomerase (Supplementary Table 2).

The proteomes were also searched for nitration at Tyr and Trp residues, the major sites of such modifications [34]. Nitration was detected on 233–345 peptides in proteins from each cell donor (Supplementary Table 3), with 47–79 of these detected in at least 2 out of 3 biological replicates from any single experimental condition (i.e. unfractionated, CF1, CF2 or CF3). Of these, 23 peptides covering 25 putative nitration sites were reproducibly detected and validated in at least 2 cell donors (Table 2, Fig. 6), indicating that these are major sites of nitration, with these being present at 17 Tyr and 8 Trp residues (Fig. 6). Tyr nitration sites were detected on 16 different proteins with 8 of these being included in a previous Tyr nitration database [35], including elongation factor 1-alpha, endoplasmic reticulum lectin 1, eukaryotic translation initiation factor 5A-2, heat shock protein HSP 90, moesin, profilin, T-complex protein 1 and tubulin. For proteins such as A-kinase anchor protein 9, beta-actin, dihydropyrimidinase and guanine nucleotide-binding protein G(I)/G(S)/G(T), similar but non-identical matches were found in this database [35]. Proteins not included in the database include armadillo repeat-containing protein 6, interleukin-1 receptor-associated kinase and protein FAM171A1. Two proteins, moesin and tubulin alpha-1C chain feature on both the list of proteins with oxidations and nitrations. Searches for Tyr and Trp nitration were also carried out against a public endothelial cell proteomic dataset (PXD037861 [28]); these searches identified 5 common nitrated peptides between the two datasets (Table 2). Evidence for tyrosine nitration in the peptide $_{149}$TTGIVMDSGDGVTHIVPIYEGYALPHAILR$_{178}$ from beta-actin-like protein 2 was also obtained when we interrogated a dataset (PXD006675) containing proteomics MS data for endothelial cells isolated from the atrium of patients undergoing cardiac surgery [29].

4. Discussion

In this study, quantitative LC-MS/MS proteomics was performed on HCAEC isolated from three donors. Robust and in-depth data were obtained from three biological replicates from each of the three cell donors, providing high quality proteome data. Each sample was analyzed both with, and without, SEC fractionation. The SEC pre-fractionation resulted in an increase in the number of proteins identified when using DIA data acquisition. This increase in number of identifications has to be balanced against the more complex and time-consuming

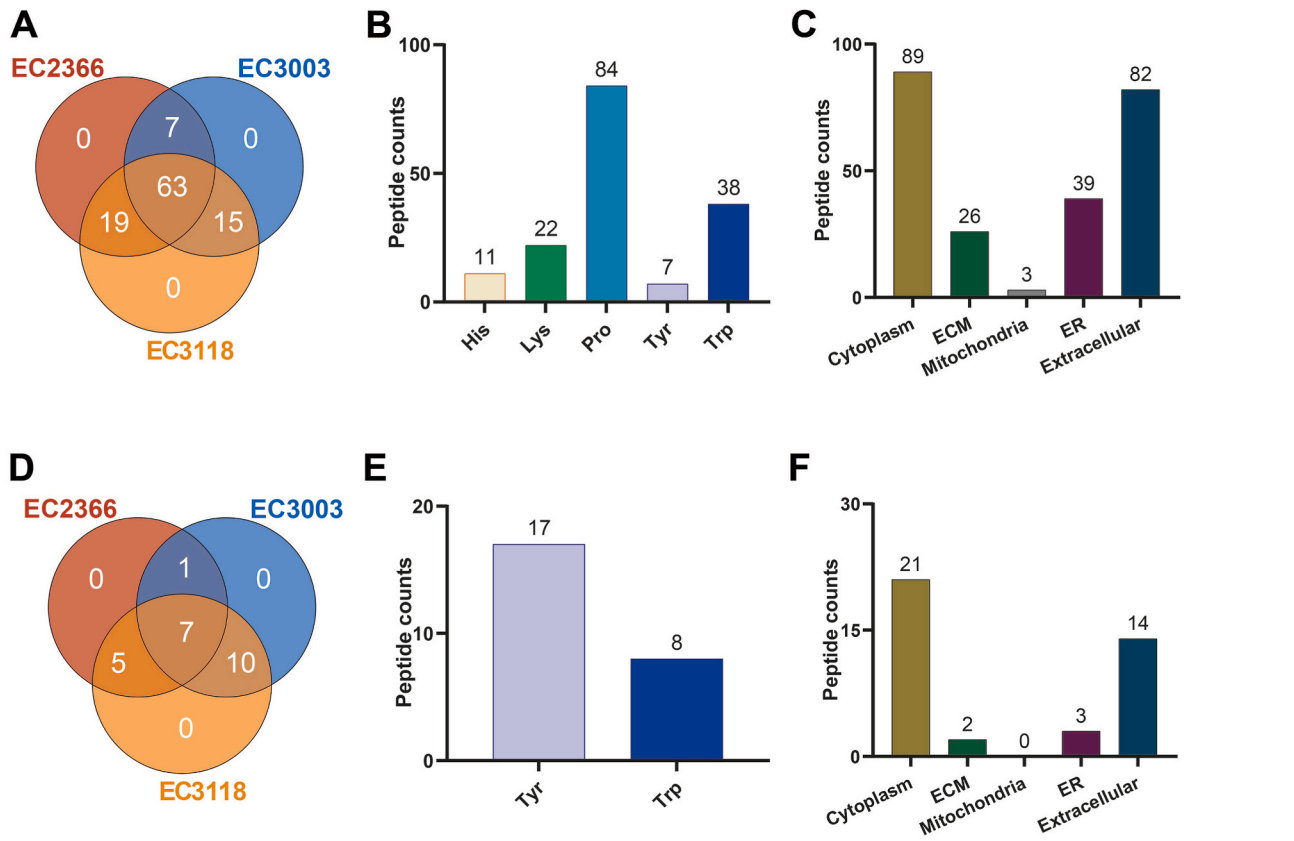

Fig. 6. (A) Venn diagram showing validated modified peptides identified in at least two out of the three HCAEC donors, with Met-containing peptides excluded. (B) Site-specific residue assignment of validated oxidized peptides expressed as the number of peptides detected with modification at the indicated residue. (C) Cell compartment annotation of validated oxidized peptides. (D) Venn diagram showing validated nitrated peptides. (E) Site-specific residue assignment of validated nitrated peptides. (F) Cell compartment annotation of validated nitrated peptides.

sample processing, and the increased machine time needed for the analysis (3-fold, even when combined fractions are used as employed here, but potentially much more). These data also indicate the significant advantages of DIA analysis, as a greater depth and breadth of proteome coverage (i.e. total number of proteins) were observed when compared to the DDA approach. However, the latter (currently) offers significant advantages in terms of the analysis of protein modifications (PTM, see also below), where analysis of DIA data is problematic. However, this drawback of DIA may decrease or disappear with recent software developments (e.g. new versions of DIA-NN).

The SEC chromatograms, PCA, and heat map analyses all demonstrated significant clustering within the biological replicates from HCAEC isolated from a single donor, indicating good reproducibility of the methods employed, but greater differences between cells isolated from different donors (c.f. principal component analysis plot in Fig. 4A and heat map, Fig. 4B). The proteomes from HCAEC from two donors (EC3003 and EC3118) were closely aligned, whereas that from the third donor (EC2366) showed greater differences (Fig. 4B). Comparison of the proteomes revealed that the composition of ECM proteins were a significant factor in the overall proteome differences between the cells. The underlying reasons for these differences cannot be determined from the current data. It is interesting to note that the donor (EC2366), which showed the greatest divergence, was significantly older (60 years) than the other donors (31 and 38 years), suggesting that age may be a significant factor. However contributions from other factors (e.g. smoking, diabetes, BMI, hypertension, other diseases) may also play a role, and cannot be assessed, as no additional data are available on these (commercial) cell donors. These factors are clearly worthy of further investigation, though there are potential logistic problems in obtaining sufficient donor cells simultaneously.

Detailed analysis of two representative ECM proteins, collagens and laminins, revealed differences in the isoforms of these proteins between the HCAEC from different donors. Donor EC2366 again showed divergence when compared to the other donors, both with regards to the total number of ECM species detected (264 for EC2366, versus 314 and 316 for EC3003 and EC3118, respectively) and the relative amounts of different core ECM species, and particularly collagens 1A1/A2, collagen 2A1, collagen 4A1, and laminins A2 and A5. Differences were also detected in collagen 6A2, though this was less marked. These changes may be associated with known age-dependent decreases in ECM synthesis capacity [36,37], though it may also result from increased ECM degradation with age, or a combination of these two factors [37].

In the current study, multiple PTMs were detected in the proteome datasets. In general, similar modification sites in the different target proteins were mapped, although some variation between the HCAEC from each donor were detected. A large number of the modifications identified are hydroxylations at Pro residues on ECM proteins, with these being consistent with deliberate enzymatic oxidation. These were detected particularly on collagen chains, which would be expected from the key role of these PTMs in stabilizing collagen triple helical structures (Table 1) and the high abundance of this modification in these proteins ([38]; see also [39]). Pro hydroxylation was also detected on other ECM proteins, together with Lys hydroxylation [40,41], which was less abundant. The lower abundance of the latter type of modification was expected as it is often transient, with this species known to be involved in subsequent cross-links to other proteins and as a site of glycosylation [38,40,41]. These further modifications on the hydroxylated Lys residues would not be detected using the approach used in the current study.

Oxidation of Trp, Tyr and His was also observed on ECM proteins. In some cases, the site of oxidation could not be unambiguously identified,

Table 1
Summary of oxidized ECM proteins and corresponding peptides detected in at least two cell donors. The modified residue(s) are indicated in red and bold text. Key: Ox – hydroxylation or oxidation (*m/z* +15.9949); IAM – addition of acetamide at Cys (*m/z* +57.0215) from thiol group alkylation using iodoacetamide.

Protein	Accession number	Gene	Peptide (with start and end amino acid number in protein sequence)	EC2366	EC3003	EC3118
Collagen alpha-1(I) chain	P02452	COL1A1	$_{539}$GLTGSP^{Ox}GSP^{Ox}GPDGK$_{552}$	x	x	
Collagen alpha-1(I) chain	P02452	COL1A1	$_{866}$GSAGPP^{Ox}GATGFP^{Ox}GAAGR$_{882}$	x	x	
Collagen alpha-1(II) chain	P02458	COL2A1	$_{981}$GIVGLP^{Ox}GQR$_{989}$		x	x
Collagen alpha-1(II) chain	P02458	COL2A1	$_{120}$GPP^{Ox}GPQGPAGEQGPR$_{134}$		x	x
Collagen alpha-1(IV) chain	P02462	COL4A1	$_{397}$GFP^{Ox}GTSLP^{Ox}GPSGR$_{409}$		x	x
Collagen alpha-1(IV) chain	P02462	COL4A1	$_{586}$GPP^{Ox}GGVGFP^{Ox}GSR$_{597}$	x	x	x
Collagen alpha-1(V) chain	P20908	COL5A1	$_{1422}$TGPIGPQGAP^{Ox}GKP^{Ox}GPDGLR$_{1440}$		x	x
Collagen alpha-2(I) chain	P08123	COL1A2	$_{592}$GP^{Ox}PGESGAAGPTGPIGSR$_{609}$	x	x	
Collagen alpha-2(IV) chain	P08572	COL4A2	$_{728}$EGFP^{Ox}GPP^{Ox}GFIGPR$_{740}$	x	x	x
Collagen alpha-2(IV) chain	P08572	COL4A2	$_{771}$GLP^{Ox}GEVLGAQP^{Ox}GPR$_{784}$	x	x	x
Collagen alpha-2(IV) chain	P08572	COL4A2	$_{109}$GVSGFP^{Ox}GADGIP^{Ox}GHP^{Ox}GQGGPR$_{129}$	x	x	x
Collagen alpha-2(IV) chain	P08572	COL4A2	$_{1672}$YSFWLTTIP^{Ox}*EQSFQGSPSADTLKAGLIR$_{1699}$		x	x
Collagen alpha-2(V) chain	P05997	COL5A2	$_{573}$GLTGNP^{Ox}GVQGPEGK$_{586}$	x	x	x
Collagen alpha-2(V) chain	P05997	COL5A2	$_{900}$GTQGPP^{Ox}GATGFP^{Ox}GSAGR$_{916}$	x	x	x
Collagen alpha-2(V) chain	P05997	COL5A2	$_{272}$NGNP^{Ox}GEVGFAGSP^{Ox}GAR$_{287}$	x	x	x
EGF-containing fibulin-like extracellular matrix protein 1	Q12805	EFEMP1	$_{300}$TSSYLC^{IAM}QYQC^{IAM}VNEP^{Ox}*GK$_{315}$	x	x	x
Endoplasmin	P14625	HSP90B1	$_{271}$YSQFINFPIYVW$^{Ox\,\#}$SSK$^{Ox}{}_{285}$	x	x	x
Fibrillin-1	P35555	FBN1	$_{1084}$GQC^{IAM}VNTP^{Ox}*GDFEC^{IAM}K$_{1096}$		x	x
Fibronectin	P02751	FN1	$_{2002}$FLATTPNSLLVSW$^{Ox\#}$QP^{Ox}PR$_{2018}$	x		x
Fibronectin	P02751	FN1	$_{1821}$FTQVTP^{Ox}*TSLSAQW$^{Ox\#}$TPPNVQLTGYR$_{1844}$	x	x	x
Laminin subunit alpha-4	A0A0A0MQS9	LAMA4	$_{871}$RPELTETADQFILY^{Ox}LGSK$_{888}$	x	x	x
Plasminogen activator inhibitor 1	P05121	SERPINE1	$_{267}$EVPLSALTNILSAQLISH^{Ox}*W^{Ox}*K$^{\$}{}_{286}$	x	x	x
Plasminogen activator inhibitor 1	P05121	SERPINE1	$_{157}$FIINDW$^{Ox\#}$VK$^{Ox}{}_{164}$	x	x	x
Plasminogen activator inhibitor 1	P05121	SERPINE1	$_{186}$LVLVNALYFNGQW$^{Ox\#}$K$^{Ox}{}_{199}$	x	x	x
Procollagen-lysine, 2-oxoglutarate 5-dioxygenase 1	Q02809	PLOD1	$_{55}$IQALGLGEDWNVEK^{Ox}*GTSAGGGQK$_{77}$	x	x	x
Protein-glutamine gamma-glutamyltransferase 4	P49221	TGM4	$_{46}$LVLNQP^{Ox}LQSY^{Ox}H^{Ox}QLK$_{59}$	x	x	x
Vimentin	P08670	VIM	$_{283}$NLQEAEEW^{Ox}Y^{Ox}K$^{\$}{}_{292}$	x	x	x

[a]Possibly Trp dioxidation instead of two monooxidations.
[b]Site assignment ambiguous.
[c]Peptide also detected with single oxidation.

including on peptides from EGF-containing fibulin-like extracellular matrix protein 1, endoplasmin, fibrillin-1, plasminogen activator inhibitor-1, procollagen-lysine and 2-oxoglutarate 5-dioxygenase 1. In many of these examples, oxidation appears to occur at two neighboring (or nearby) residues, often involving at least one Trp residue, and these may potentially be di-oxygenations at Trp (e.g. to give *N*-formylkynurenine or hydroperoxides) rather than two mono-oxygenations. Of particular note are the multiple modifications detected on plasminogen activator inhibitor-1, where modifications were detected at 3 different sites. Oxidation was also detected on fibronectin, and laminin subunit alpha-4, which are both abundant and established targets of oxidants [42–46]. Reaction with adventitious oxidants rather than deliberate enzyme-mediated reactions is the likely source of these modifications. Interestingly, both the fibronectin sites detected as oxidized in the current study (Trp1742 and Trp1923), were also detected as modified on exposure of fibronectin to reagent hypochlorous acid (HOCl) [42]. Both modified residues lie within the Heparin II binding domain, suggesting that oxidation at these sites may be of functional importance.

Oxidation of cellular proteins was also detected, which may be related to their abundance, intracellular location or function. There was evidence for hydroxylation of Pro, and oxidation of Lys, His, Trp and Tyr residues (Supplementary Table 2). As with some of the ECM proteins, the exact location of the modifications could not be determined for some species (as above). A limited number of proteins, including the key metabolic and signaling enzyme glyceraldehyde-3-phosphate dehydrogenase (GAPDH), metallothionein-2, moesin, protein disulfide-isomerase (P4HB), protein disulfide isomerase A3, thioredoxin domain-containing protein 5, and transgelin-2, were modified at multiple sites, as shown by the detection of several tryptic peptides containing PTMs from each of these proteins. Protein disulfide-isomerase isoforms appear to be important targets, with evidence for the modification of 10 peptides across 3 isoforms. Whilst some of these modifications have been assigned as Pro hydroxylations, it is possible that modification of (common) neighboring Trp residues could account for the mass change. This uncertainty cannot be resolved from the current data due to the limited fragments detected from these peptide sequences. Several of the oxidized residues identified in the protein disulfide-isomerases and thioredoxin, are located close to the active site CXXC motif involved in thiol-disulfide exchange reactions. Consequently, these modifications may impact on protein activity, though this has not been examined. However it has previously been demonstrated that the conserved Trp31 residue in thioredoxin [47], identified here as being oxidized, plays a critical role in disulfide bond reduction.

Nitration was also detected on a limited number of proteins at Tyr and Trp residues with the former being more numerous. This is consistent with previous data and appears to occur irrespective of the Tyr:Trp ratio, indicating that Tyr nitration is more favorable [34,48]. This has been ascribed to a decreased extent of competition from other reactions (e.g. less rapid addition of O_2 to the Tyr phenoxyl radical compared to Trp indolyl species [48]). With moesin and tubulin alpha-1C chain, there was evidence for both oxidation and nitration but on different peptides,

Table 2
Summary of modified peptides and parent proteins detected across the three HCAEC donors and comparison with those detected previously for corresponding smooth muscle cells (SMC) reported in previous studies. The modified residue(s) are indicated in red bold text. Key: Nit – nitration (*m/z* +44.9851); IAM – addition of acetamide at Cys (*m/z* +57.0215) from thiol group alkylation using iodoacetamide; Ox - oxidation.

				EC			SMC
Protein	**Accession number**	**Gene**	**Peptide (with start and end amino acid number in protein sequence)**	**2366**	**3003**	**3118**	**1522**
A-kinase anchor protein 9	Q99996	AKAP9	$_{3669}$AEAEV**Y^{Nit}**KLKAELR$_{3681}$		x	x	x[a]
Armadillo repeat-containing protein 6	Q6NXE6	ARMC6	$_{129}$FLAAQKGA**Y^{Nit}**PIIFTA**W^{Nit}**K^{S}$_{145}$	x		x	
Beta-actin-like protein 2	Q562R1	ACTBL2	$_{293}$DLYANTVLSGGSTM**Y^{Nit}**PGIADR$_{313}$		x	x	x[b]
Beta-actin-like protein 2	Q562R1	ACTBL2	$_{149}$TTGIVMDSGDGVTHIVPI**Y^{Nit}**EGYALPHAILR^{S}*$_{178}$	x	x	x	x[b]
Dihydropyrimidinase	Q14117	DPYS	$_{446}$VV**Y^{Nit}**EAGVFSVTAGDGK$_{461}$	x	x	x	
Dihydropyrimidinase-related protein 4	O14531	DPYSL4	$_{24}$IVNDDQSF**Y^{Nit}**ADVHVEDGLIK$_{43}$	x	x		
Elongation factor 1-alpha 1[#]	P68104	EEF1A1	$_{135}$EHALLA**Y^{Nit}**TLGVK$_{146}$		x	x	
Elongation factor 1-alpha 1[#]	P68104	EEF1A1	$_{181}$IGYNPDTVAFVPISG**W^{Nit}**NGDNMLEPSANMPWFK$_{212}$	x	x	x	x[a]
Endoplasmic reticulum lectin 1[#]	Q96DZ1	ERLEC1	$_{77}$**Y^{Nit}**K**C^{IAM}**ILPLVTSGDEEEEKDYK$_{96}$		x	x	
Eukaryotic translation initiation factor 5A-2[#]	Q9GZV4	EIF5A2	$_{2}$ADEIDFTTGDAGASST**Y^{Nit}**PMQ**C^{IAM}**SALR$_{26}$	x	x	x	
Guanine nucleotide-binding protein G(I)/G(S)/G(T) subunit beta-3	P16520	GNB3	$_{315}$VS**C^{IAM}**LGVTADGMAVATGS**W^{Nit}**DSFLK$_{337}$		x	x	x[b]
Heat shock protein HSP 90-alpha[#]	P07900	HSP90AA1	$_{420}$**C^{IAM}**LELFTELAEDKEN**Y^{Nit}**KK$_{436}$		x	x	x[b]
Heat shock protein HSP 90-alpha[#]	P07900	HSP90AA1	$_{592}$LVTSP**C^{IAM}C^{IAM}**IVTSTY^{Nit}GW^{R}TANMER$_{612}$		x	x	
Heat shock protein HSP 90-beta[#]	P08238	HSP90AB1	$_{584}$LVSSP**C^{IAM}C^{IAM}**IVTSTY^{Nit}GW^{R}TANMER$_{604}$	x		x	
Interleukin-1 receptor-associated kinase 4	Q9NWZ3	IRAK4	$_{339}$FAQTVMTSRIVGTTA**Y^{Nit}**MAPEALR$_{361}$		x	x	
Moesin[#]	P26038	MSN	$_{194}$IAQDLEMYGVNY**^{Nit}**FSIK$_{209}$		x	x	
Oxysterol-binding protein-related protein 9	Q96SU4	OSBPL9	$_{430}$MVQVVK**W^{Nit}Y^{Nit}**LSAFHAGR$_{445}$	x		x	x[b]
Probable phospholipid-transporting ATPase VA	O60312	ATP10A	$_{1144}$DVPANVLLTNPQL**Y^{Nit}**K^{S}$_{1158}$	x		x	
Profilin-1[#]	P07737	PFN1	$_{2}$AG**W^{Nit}**NAY^{R}IDNL**M^{Ox}**ADGT**C^{IAM}**QDAAIVGYK^{S}$_{38}$	x	x	x	x[a]
Protein FAM171A1	Q5VUB5	FAM171A1	$_{475}$EGYESSGNDD**Y^{Nit}**R$_{486}$		x	x	
T-complex protein 1 subunit alpha[#]	P17987	TCP1	$_{482}$NLK**W^{Nit}**IGLDLSNGK$_{494}$	x	x	x	x[b]
Translationally-controlled tumor protein	A0A0B4J2C3	TPT1	$_{178}$NP**C^{IAM}**AF**C^{IAM}**LSL**W^{Nit}**R$_{188}$	x		x	
Tubulin alpha-1C chain[#]	Q9BQE3	TUBA1C	$_{374}$AV**C^{IAM}**MLSNTTAVAEA**W^{Nit}**AR^{S}$_{390}$	x	x	x	x[b]

[a]Identified in smooth muscle cells without ONOOH exposure in Ref. [23].
[b]Identified in smooth muscle cells exposed to ONOOH in Ref. [23].
[c]Listed as a Tyr nitrated protein in Ref. [35].
[d]Identified in PXD037861 [28].
[e]Identified in PXD006675 [29].
[f]Annotated as nitrated residue in some spectra.

and sites. Interestingly, a number of proteins that have been previously reported as being sensitive to nitration, including prostaglandin I2 (prostacyclin) synthase [49,50] and mitochondrial superoxide dismutase (SOD2) [51,52], were either not detected in the proteome datasets in either their native or any modified forms (prostaglandin I2 synthase), or not detected in their nitrated form (SOD2). In the latter case, all three isoforms were detected as unmodified species.

As with the oxidations observed, a small number of proteins were nitrated at multiple sites, including beta actin-like protein 2, elongation factor 1-alpha 1, and heat shock proteins HSP 90-alpha and -beta (Table 2). These data indicate that some proteins are more prone to nitration than others, and that some specific sites are very sensitive to nitration. As with the oxidations, this may be due to their abundance, or subcellular location. Of particular interest, is the observation that 10 of these nitrated proteins were also detected in a previous study on human coronary smooth muscle cells (HCASMC) exposed to ONOOH/ONOO^{-} [23], suggesting that there are common nitration targets in the vascular proteome. Five of the peptides (those from beta-actin-like protein 2, elongation factor 1-alpha 1, profilin-1, T-complex protein 1 subunit alpha, tubulin alpha-1C chain) detected for all three HCAEC donors were also detected in a corresponding HCASMC dataset [23], suggesting that these are common targets across different vascular cells. This consistent modification strongly suggests that these proteins are major nitration targets even under basal (no added oxidant) conditions. This conclusion is reinforced by a search of an existing public endothelial cell protein dataset [28], where 5 common nitrated peptides (from armadillo repeat-containing protein 6, beta-actin-like protein 2, probable phospholipid-transporting ATPase VA, profilin-1 and tubulin alpha-1C chain) were detected across these datasets (Table 2). Thus, 3 nitrated peptides (from beta-actin-like protein 2, profilin-1 and tubulin alpha-1C chain) have been detected as common across all three datasets. The identification of nitrated beta-actin-like protein 2 in endothelial cells derived from human cardiac tissue underpins the physiological relevance of these findings [29].

Several of the nitrated proteins identified from the HCAEC are known to play an important role in regulation of cytoskeletal dynamics and vascular tone. For example, nitration can block polymerization of β-actin and has been observed following TNFα-mediated exposure to ONOOH in vascular endothelial cells [53]. Nitration of beta-actin and HSP90 may be influenced by the close association of these proteins with eNOS, a significant source of NO$^{\cdot}$, and hence probably peroxynitrous acid [54]. Furthermore, several of the other identified nitrated proteins are known to interact with actin, including moesin, profilin, T-complex protein 1, and translationally-controlled tumor protein. Nitration of the cytoskeletal protein tubulin can regulate dynein dynamics and microtubule formation, with Tyr449 in the alpha chain being an established target [55]. Here we identified nitration of Trp388 in tubulin alpha-1C chain in all three HCAEC donors (as well as in HCASMC exposed to ONOOH [23]) and this modification may show similar functional consequences. Nitration at Tyr354 was also detected on interleukin-1 receptor-associated kinase 4 (IRAK-4), a key regulatory molecule which modulates nuclear factor-κB (NFκB) signaling [56]. Consistent with this detection, a previous study has reported that eNOS-mediated nitration of IRAK-4 modulates this pathway [56].

Multiple different processes are likely to contribute to the modifications detected in the current study. The oxidation of Pro and Lys is likely to arise from the enzymatic activity of multiple enzymes and is an intentional PTM required for biological function (e.g. at Pro to stabilize collagen triple helices, or at Lys for protein cross-linking and sugar attachment [38,40,41]). In contrast, the oxidative modifications at Trp, Tyr and His, and the nitration of Trp and Tyr, probably arise from unintended processes. Whilst multiple processes are known to generate

oxidative modifications (reviewed [31,33]), the nitration is likely to arise from nitrating species (e.g. peroxynitrous acid/peroxynitrite, $NO_2^{\cdot}$, N_2O_3 [34,57]) arising from the enzymatic activity of eNOS, a constitutive enzyme of HCAEC, and critical for the biological vasorelaxation activity of these cells. Peroxynitrous acid/peroxynitrite is also a well-established oxidant, and may contribute to the oxidations detected at Trp, Tyr and His [34,57]. $NO_2^{\cdot}$ can also be formed from the reaction of nitrite (NO_2^-) with activated peroxidase enzymes (e.g. myeloperoxidase (MPO) and peroxidasin (PXDN) [58–60]), and this radical can generate nitrated products from Tyr and Trp residues [34,57]. However, there are few data supporting the presence of MPO in primary endothelial cells *ex vivo*, although MPO can be detected in arterial wall ECs *in vivo* at sites of inflammation [61]. Thus, MPO is unlikely to be a significant source of nitration in the current study. In contrast, PXDN is expressed in ECs, and has been reported to be essential for EC survival [62]. This enzyme is therefore a potential candidate for the source of the observed nitration, in addition to peroxynitrous acid/peroxynitrite or N_2O_3. Further studies are required to examine these possibilities.

This study has several strengths and limitations. The use of 3 biological replicates from three different HCAEC donors has allowed both a broad and in-depth analysis of the cellular and ECM proteomes of these primary cells, whose dysfunction is of major importance in multiple human pathologies. Analysis of the data using the gene ontology (GO) term 'Cellular Component' shows that good coverage of both intra- and extra-cellular proteins, and also species from different cellular compartments has been achieved (Supplementary Data File 2). Thus proteins have been detected from all major organelles (e.g. nuclear, mitochondrial, cytosol, lysosomal, endoplasmic reticulum, Golgi apparatus, peroxisomes, vesicles, membrane species, etc), as well as many enzyme complexes (e.g. respiratory and electron-transport chains) and the extracellular matrix that surrounds and supports cells. The current datasets therefore provide an important basis for studying changes that occur during the development of disease (e.g. atherosclerosis and aortic aneurysms). The data on ECM changes – a topic commonly neglected in proteomic studies (though see Ref. [21]) – may also be of major importance given the growing realization that ECM changes are of critical importance in both the above diseases, and also the many pathologies involving fibrosis [63,64]. This study also provides an in-depth analysis of the occurrence, sites and protein targets of endogenous oxidation and nitration in this cell type, and revealed a number of specific and sensitive targets of these processes, with some of these validated using other available datasets, and against data for related primary coronary artery smooth muscle cells [23].

It would clearly be advantageous to examine larger numbers of HCAEC samples from additional cell donors, but this would be associated with significant technical and cost limitations associated with the processing and running of large numbers of samples. The lack of additional (clinical and lifestyle) data on the donors is a significant limitation, and there would be obvious benefits in examining donors of different ages in the light of the observed clustering of the data from the two younger donors compared to the single older donor, to determine whether subject age is a major factor. In addition, larger number of donors would allow potential differences arising from biological sex, ethnicity and lifestyle factors to be discerned.

It should also be noted that there are a significant number of limitations arising from the experimental set-ups employed. These include the use of cultures generated under 21 % O_2, which does not reflect biological reality (endothelial cells in major blood vessels are typically exposed to ~ 13 % O_2), the use of static cultures (i.e. absence of flow) and the absence of other cell types which may modulate cell behavior. Furthermore, the post-translational modifications searched for exclude modifications at Cys residues. This is a (partial) consequence of the elimination of unstable modifications at Cys as a result of the reduction and alkylation steps carried out during sample processing that were required to obtain high sequence coverage. Furthermore, the large number of products that can be generated from this residue massively increases the computational time and power required to carry out comprehensive searches. However, this would be a critical avenue to follow up on, in future studies.

CRediT authorship contribution statement

Shuqi Xu: Writing – original draft, Visualization, Validation, Methodology, Investigation, Funding acquisition, Formal analysis. **Christine Y. Chuang:** Writing – review & editing, Supervision, Project administration, Methodology, Investigation, Formal analysis. **Clare L. Hawkins:** Writing – review & editing, Supervision, Resources, Project administration, Formal analysis. **Per Hägglund:** Writing – review & editing, Validation, Supervision, Resources, Methodology, Formal analysis, Data curation. **Michael J. Davies:** Writing – review & editing, Writing – original draft, Supervision, Resources, Project administration, Funding acquisition, Conceptualization.

Declaration of competing interest

MJD declares consultancy contracts with Novo Nordisk A/S. This funder had no role in the design of the study; in the collection, analyses, or interpretation of data; in the writing of the manuscript, or in the decision to publish the results. The other authors declare no conflict of interest.

Acknowledgements

This work was supported by the Novo Nordisk Foundation (Laureate Continuation Grant: NNF20SA0064214 to MJD) and the China Scholarship Council (PhD scholarship 201806270237 to Shuqi Xu). We thank Dr. Lasse G. Lorentzen for valuable scientific discussions.

Appendix A. Supplementary data

Supplementary data to this article can be found online at https://doi.org/10.1016/j.redox.2025.103524.

Data availability

The mass spectrometry proteomics data have been deposited to the ProteomeXchange Consortium via the PRIDE partner repository with the dataset identifier PXD056929.

References

[1] E. Trimm, K. Red-Horse, Vascular endothelial cell development and diversity, Nat. Rev. Cardiol. 20 (3) (2023) 197–210, https://doi.org/10.1038/s41569-022-00770-1.
[2] A.L. Baldwin, G. Thurston, Mechanics of endothelial cell architecture and vascular permeability, Crit. Rev. Biomed. Eng. 29 (2) (2001) 247–278, https://doi.org/10.1615/critrevbiomedeng.v29.i2.20.
[3] A. Kruger-Genge, A. Blocki, R.P. Franke, F. Jung, Vascular endothelial cell biology: an update, Int. J. Mol. Sci. 20 (18) (2019), https://doi.org/10.3390/ijms20184411.
[4] D. Mehta, A.B. Malik, Signaling mechanisms regulating endothelial permeability, Physiol. Rev. 86 (1) (2006) 279–367, https://doi.org/10.1152/physrev.00012.2005.
[5] N. Wettschureck, B. Strilic, S. Offermanns, Passing the vascular barrier: endothelial signaling processes controlling extravasation, Physiol. Rev. 99 (3) (2019) 1467–1525, https://doi.org/10.1152/physrev.00037.2018.
[6] V.W. van Hinsbergh, Endothelium–role in regulation of coagulation and inflammation, Semin. Immunopathol. 34 (1) (2012) 93–106, https://doi.org/10.1007/s00281-011-0285-5.
[7] H.A. Hadi, C.S. Carr, J. Al Suwaidi, Endothelial dysfunction: cardiovascular risk factors, therapy, and outcome, Vasc. Health Risk Manag. 1 (3) (2005) 183–198.
[8] T. Hsu, H.H. Nguyen-Tran, M. Trojanowska, Active roles of dysfunctional vascular endothelium in fibrosis and cancer, J. Biomed. Sci. 26 (1) (2019) 86, https://doi.org/10.1186/s12929-019-0580-3.
[9] P. Rajendran, T. Rengarajan, J. Thangavel, Y. Nishigaki, D. Sakthisekaran, G. Sethi, I. Nishigaki, The vascular endothelium and human diseases, Int. J. Biol. Sci. 9 (10) (2013) 1057–1069, https://doi.org/10.7150/ijbs.7502.

[10] M.A. Gimbrone Jr., G. Garcia-Cardena, Endothelial cell dysfunction and the pathobiology of atherosclerosis, Circ. Res. 118 (4) (2016) 620–636, https://doi.org/10.1161/CIRCRESAHA.115.306301.
[11] A.J. Lusis, Atherosclerosis, Nature 407 (2000) 233–241, https://doi.org/10.1038/35025203.
[12] R. Ross, Atherosclerosis–an inflammatory disease, N. Engl. J. Med. 340 (1999) 115–126, https://doi.org/10.1056/NEJM199901143400207.
[13] P. Libby, P.M. Ridker, A. Maseri, Inflammation and atherosclerosis, Circulation 105 (9) (2002) 1135–1143, https://doi.org/10.1161/hc0902.104353.
[14] G.R. Geovanini, P. Libby, Atherosclerosis and inflammation: overview and updates, Clin. Sci. (Lond.) 132 (12) (2018) 1243–1252, https://doi.org/10.1042/CS20180306.
[15] G.K. Hansson, P. Libby, I. Tabas, Inflammation and plaque vulnerability, J. Intern. Med. 278 (5) (2015) 483–493, https://doi.org/10.1111/joim.12406.
[16] P. Libby, The biology of atherosclerosis comes full circle: lessons for conquering cardiovascular disease, Nat. Rev. Cardiol. 18 (10) (2021) 683–684, https://doi.org/10.1038/s41569-021-00609-1.
[17] D.A. Chistiakov, I.A. Sobenin, A.N. Orekhov, Vascular extracellular matrix in atherosclerosis, Cardiol. Rev. 21 (6) (2013) 270–288, https://doi.org/10.1097/CRD.0b013e31828c5ced.
[18] S. Holm Nielsen, L. Jonasson, K. Kalogeropoulos, M.A. Karsdal, A.L. Reese-Petersen, U. Auf dem Keller, F. Genovese, J. Nilsson, I. Goncalves, Exploring the role of extracellular matrix proteins to develop biomarkers of plaque vulnerability and outcome, J. Intern. Med. 287 (5) (2020) 493–513, https://doi.org/10.1111/joim.13034.
[19] S.R. Langley, K. Willeit, A. Didangelos, L.P. Matic, P. Skroblin, J. Barallobre-Barreiro, M. Lengquist, G. Rungger, A. Kapustin, L. Kedenko, C. Molenaar, R. Lu, T. Barwari, G. Suna, X. Yin, B. Iglseder, B. Paulweber, P. Willeit, J. Shalhoub, G. Pasterkamp, A.H. Davies, C. Monaco, U. Hedin, C.M. Shanahan, J. Willeit, S. Kiechl, M. Mayr, Extracellular matrix proteomics identifies molecular signature of symptomatic carotid plaques, J. Clin. Investig. 127 (4) (2017) 1546–1560, https://doi.org/10.1172/JCI86924.
[20] S.J. Parker, L. Chen, W. Spivia, G. Saylor, C. Mao, V. Venkatraman, R. J. Holewinski, M. Mastali, R. Pandey, G. Athas, G. Yu, Q. Fu, D. Troxlair, R. Vander Heide, D. Herrington, J.E. Van Eyk, Y. Wang, Identification of putative early atherosclerosis biomarkers by unsupervised deconvolution of heterogeneous vascular proteomes, J. Proteome Res. 19 (7) (2020) 2794–2806, https://doi.org/10.1021/acs.jproteome.0c00118.
[21] L.G. Lorentzen, K. Yeung, N. Eldrup, J.P. Eiberg, H.H. Sillesen, M.J. Davies, Proteomic analysis of the extracellular matrix of human atherosclerotic plaques shows marked changes between plaque types, Matrix Biol. 21 (2024) 100141, https://doi.org/10.1016/j.mbplus.2024.100141.
[22] M. Wierer, M. Prestel, H.B. Schiller, G. Yan, C. Schaab, S. Azghandi, J. Werner, T. Kessler, R. Malik, M. Murgia, Z. Aherrahrou, H. Schunkert, M. Dichgans, M. Mann, Compartment-resolved proteomic analysis of mouse aorta during atherosclerotic plaque formation reveals osteoclast-specific protein expression, Mol. Cell. Proteomics 17 (2) (2018) 321–334, https://doi.org/10.1074/mcp.RA117.000315.
[23] S. Xu, C.Y. Chuang, C.L. Hawkins, P. Hagglund, M.J. Davies, Identification and quantification of protein nitration sites in human coronary artery smooth muscle cells in the absence and presence of peroxynitrous acid/peroxynitrite, Redox Biol. 64 (2023) 102799, https://doi.org/10.1016/j.redox.2023.102799.
[24] J. Rappsilber, M. Mann, Y. Ishihama, Protocol for micro-purification, enrichment, pre-fractionation and storage of peptides for proteomics using stagetips, Nat. Protoc. 2 (8) (2007) 1896–1906, https://doi.org/10.1038/nprot.2007.261.
[25] F. Meier, A.D. Brunner, S. Koch, H. Koch, M. Lubeck, M. Krause, N. Goedecke, J. Decker, T. Kosinski, M.A. Park, N. Bache, O. Hoerning, J. Cox, O. Rather, M. Mann, Online parallel accumulation-serial fragmentation (PASEF) with a novel trapped ion mobility mass spectrometer, Mol. Cell. Proteomics 17 (12) (2018) 2534–2545, https://doi.org/10.1074/mcp.TIR118.000900.
[26] F. Meier, A.D. Brunner, M. Frank, A. Ha, I. Bludau, E. Voytik, S. Kaspar-Schoenefeld, M. Lubeck, O. Raether, N. Bache, R. Aebersold, B.C. Collins, H.L. Rost, M. Mann, DIA-PASEF: parallel accumulation-serial fragmentation combined with data-independent acquisition, Nat. Methods 17 (12) (2020) 1229–1236, https://doi.org/10.1038/s41592-020-00998-0.
[27] V. Demichev, L. Szyrwiel, F. Yu, G.C. Teo, G. Rosenberger, A. Niewienda, D. Ludwig, J. Decker, S. Kaspar-Schoenefeld, K.S. Lilley, M. Mulleder, A. I. Nesvizhskii, M. Ralser, DIA-PASEF data analysis using Fragpipe and DIA-NN for deep proteomics of low sample amounts, Nat. Commun. 13 (1) (2022) 3944, https://doi.org/10.1038/s41467-022-31492-0.
[28] A. Frolov, A. Lobov, M. Kabilov, B. Zainullina, A. Tupikin, D. Shishkova, V. Markova, A. Sinitskaya, E. Grigoriev, Y. Markova, A. Kutikhin, Multi-omics profiling of human endothelial cells from the coronary artery and internal thoracic artery reveals molecular but not functional heterogeneity, Int. J. Mol. Sci. 24 (19) (2023), https://doi.org/10.3390/ijms241915032.
[29] S. Doll, M. Dressen, P.E. Geyer, D.N. Itzhak, C. Braun, S.A. Doppler, F. Meier, M. A. Deutsch, H. Lahm, R. Lange, M. Krane, M. Mann, Region and cell-type resolved quantitative proteomic map of the human heart, Nat. Commun. 8 (1) (2017) 1469, https://doi.org/10.1038/s41467-017-01747-2.
[30] X. Shao, C.D. Gomez, N. Kapoor, J.M. Considine, C. Grams, Y.T. Gao, A. Naba, Matrisomedb 2.0: 2023 updates to the ECM-protein knowledge database, Nucleic Acids Res. 51 (D1) (2023) D1519–D1530, https://doi.org/10.1093/nar/gkac1009.
[31] C.L. Hawkins, M.J. Davies, Detection, identification and quantification of oxidative protein modifications, J. Biol. Chem. 294 (2019) 19683–19708, https://doi.org/10.1074/jbc.REV119.006217.
[32] A.M. Salo, J. Myllyharju, Prolyl and lysyl hydroxylases in collagen synthesis, Exp. Dermatol. 30 (1) (2021) 38–49, https://doi.org/10.1111/exd.14197.
[33] M.J. Davies, Protein oxidation and peroxidation, Biochem. J. 473 (2016) 805–825, https://doi.org/10.1042/BJ20151227.
[34] G. Ferrer-Sueta, N. Campolo, M. Trujillo, S. Bartesaghi, S. Carballal, N. Romero, B. Alvarez, R. Radi, Biochemistry of peroxynitrite and protein tyrosine nitration, Chem. Rev. 118 (3) (2018) 1338–1408, https://doi.org/10.1021/acs.chemrev.7b00568.
[35] I. Griswold-Prenner, A.K. Kashyap, S. Mazhar, Z.W. Hall, H. Fazelinia, H. Ischiropoulos, Unveiling the human nitroproteome: protein tyrosine nitration in cell signaling and cancer, J. Biol. Chem. 299 (8) (2023) 105038, https://doi.org/10.1016/j.jbc.2023.105038.
[36] J.K. Kular, S. Basu, R.I. Sharma, The extracellular matrix: structure, composition, age-related differences, tools for analysis and applications for tissue engineering, J. Tissue Eng. 5 (2014) 2041731414557112, https://doi.org/10.1177/2041731414557112.
[37] C. Statzer, J.Y.C. Park, C.Y. Ewald, Extracellular matrix dynamics as an emerging yet understudied hallmark of aging and longevity, Aging Dis 14 (3) (2023) 670–693, https://doi.org/10.14336/AD.2022.1116.
[38] R.A. Berg, D.J. Prockop, The thermal transition of a non-hydroxylated form of collagen. Evidence for a role for hydroxyproline in stabilizing the triple-helix of collagen, Biochem. Biophys. Res. Commun. 52 (1) (1973) 115–120, https://doi.org/10.1016/0006-291x(73)90961-3.
[39] K.C. Yang-Jensen, S.M. Jørgnsen, C.Y. Chuang, M.J. Davies, Modification of extracellular matrix proteins by oxidants and electrophiles, Biochem. Soc. Trans. (2024), https://doi.org/10.1042/BST20230860. BST20230860.
[40] M. Yamauchi, M. Sricholpech, Lysine post-translational modifications of collagen, Essays Biochem. 52 (2012) 113–133, https://doi.org/10.1042/bse0520113.
[41] M. Yamauchi, M. Terajima, M. Shiiba, Lysine hydroxylation and cross-linking of collagen, Methods Mol. Biol. 1934 (2019) 309–324, https://doi.org/10.1007/978-1-4939-9055-9_19.
[42] T. Nybo, H. Cai, C.Y. Chuang, L.F. Gamon, A. Rogowska-Wrzesinska, M.J. Davies, Chlorination and oxidation of human plasma fibronectin by myeloperoxidase-derived oxidants, and its consequences for smooth muscle cell function, Redox Biol. 19 (2018) 388–400, https://doi.org/10.1016/j.redox.2018.09.005.
[43] T. Nybo, S. Dieterich, L.F. Gamon, C.Y. Chuang, A. Hammer, G. Hoefler, E. Malle, A. Rogowska-Wrzesinska, M.J. Davies, Chlorination and oxidation of the extracellular matrix protein laminin and basement membrane extracts by hypochlorous acid and myeloperoxidase, Redox Biol. 20 (2019) 496–513, https://doi.org/10.1016/j.redox.2018.10.022.
[44] L.G. Lorentzen, C.Y. Chuang, A. Rogowska-Wrzesinska, M.J. Davies, Identification and quantification of sites of nitration and oxidation in the key matrix protein laminin and the structural consequences of these modifications, Redox Biol. 24 (2019) 101226, https://doi.org/10.1016/j.redox.2019.101226.
[45] M. Mariotti, A. Rogowska-Wrzesinska, P. Hagglund, M.J. Davies, Cross-linking and modification of fibronectin by peroxynitrous acid: mapping and quantification of damage provides a new model for domain interactions, J. Biol. Chem. (2021) 100360, https://doi.org/10.1016/j.jbc.2021.100360.
[46] S. Vanichkitrungruang, C.Y. Chuang, C.L. Hawkins, A. Hammer, G. Hoefler, E. Malle, M.J. Davies, Oxidation of human plasma fibronectin by inflammatory oxidants perturbs endothelial cell function, Free Radic. Biol. Med. 136 (2019) 118–134, https://doi.org/10.1016/j.freeradbiomed.2019.04.003.
[47] G. Krause, A. Holmgren, Substitution of the conserved tryptophan 31 in Escherichia coli thioredoxin by site-directed mutagenesis and structure-function analysis, J. Biol. Chem. 266 (7) (1991) 4056–4066, https://doi.org/10.1016/S0021-9258(20)64285-5.
[48] M.J. Davies, Protein nitration in the artery wall: a contributor to cardiovascular disease? Redox Biochem. Chem. 8 (2024) 100032 https://doi.org/10.1016/j.rbc.2024.100032.
[49] M.H. Zou, M. Leist, V. Ullrich, Selective nitration of prostacyclin synthase and defective vasorelaxation in atherosclerotic bovine coronary arteries, Am. J. Pathol. 154 (5) (1999) 1359–1365, https://doi.org/10.1016/S0002-9440(10)65390-4.
[50] M.H. Zou, H. Li, C. He, M. Lin, T.J. Lyons, Z. Xie, Tyrosine nitration of prostacyclin synthase is associated with enhanced retinal cell apoptosis in diabetes, Am. J. Pathol. 179 (6) (2011) 2835–2844, https://doi.org/10.1016/j.ajpath.2011.08.041.
[51] V. Demicheli, C. Quijano, B. Alvarez, R. Radi, Inactivation and nitration of human superoxide dismutase (SOD) by fluxes of nitric oxide and superoxide, Free Radic. Biol. Med. 42 (9) (2007) 1359–1368, https://doi.org/10.1016/j.freeradbiomed.2007.01.034.
[52] L.A. MacMillan-Crow, J.P. Crow, J.D. Kerby, J.S. Beckman, J.A. Thompson, Nitration and inactivation of manganese superoxide dismutase in chronic rejection of human renal allografts, Proc. Natl. Acad. Sci. U. S. A. 93 (21) (1996) 11853–11858, https://doi.org/10.1073/pnas.93.21.11853.
[53] P. Neumann, N. Gertzberg, E. Vaughan, J. Weisbrot, R. Woodburn, W. Lambert, A. Johnson, Peroxynitrite mediates TNF-alpha-induced endothelial barrier dysfunction and nitration of actin, Am. J. Physiol. Lung Cell. Mol. Physiol. 290 (4) (2006) L674–L684, https://doi.org/10.1152/ajplung.00391.2005.
[54] Y. Ji, G. Ferracci, A. Warley, M. Ward, K.Y. Leung, S. Samsuddin, C. Leveque, L. Queen, V. Reebye, P. Pal, E. Gkaliagkousi, M. Seager, A. Ferro, Beta-actin regulates platelet nitric oxide synthase 3 activity through interaction with heat shock protein 90, Proc. Natl. Acad. Sci. U. S. A. 104 (21) (2007) 8839–8844, https://doi.org/10.1073/pnas.0611416104.
[55] J.P. Eiserich, A.G. Estevez, T.V. Bamberg, Y.Z. Ye, P.H. Chumley, J.S. Beckman, B. A. Freeman, Microtubule dysfunction by posttranslational nitrotyrosination of alpha-tubulin: a nitric oxide-dependent mechanism of cellular injury, Proc. Natl.

Acad. Sci. U. S. A. 96 (11) (1999) 6365–6370, https://doi.org/10.1073/pnas.96.11.6365.
[56] M.K. Mirza, J. Yuan, X.P. Gao, S. Garrean, V. Brovkovych, A.B. Malik, C. Tiruppathi, Y.Y. Zhao, Caveolin-1 deficiency dampens toll-like receptor 4 signaling through eNOS activation, Am. J. Pathol. 176 (5) (2010) 2344–2351, https://doi.org/10.2353/ajpath.2010.091088.
[57] B. Alvarez, R. Radi, Peroxynitrite reactivity with amino acids and proteins, Amino Acids 25 (2003) 295–311, https://doi.org/10.1007/s00726-003-0018-8.
[58] S. Xu, C.Y. Chuang, E. Malle, L.F. Gamon, C.L. Hawkins, M.J. Davies, Influence of plasma halide, pseudohalide and nitrite ions on myeloperoxidase-mediated protein and extracellular matrix damage, Free Radic. Biol. Med. 188 (2022) 162–174, https://doi.org/10.1016/j.freeradbiomed.2022.06.222.
[59] J.P. Eiserich, M. Hristova, C.E. Cross, A.D. Jones, B.A. Freeman, B. Halliwell, A. van der Vliet, Formation of nitric oxide-derived inflammatory oxidants by myeloperoxidase in neutrophils, Nature 391 (1998) 393–397, https://doi.org/10.1038/34923.
[60] B. Sevcnikar, M. Paumann-Page, S. Hofbauer, V. Pfanzagl, P.G. Furtmuller, C. Obinger, Reaction of human peroxidasin 1 compound I and compound II with one-electron donors, Arch. Biochem. Biophys. 681 (2020) 108267, https://doi.org/10.1016/j.abb.2020.108267.
[61] S. Baldus, J.P. Eiserich, A. Mani, L. Castro, M. Figueroa, P. Chumley, W. Ma, A. Tousson, T.C.R. White, D.C. Bullard, M.-L. Brennan, A.J. Lusis, K.P. Moore, B. A. Freeman, Endothelial transcytosis of myeloperoxidase confers specificity to vascular ECM proteins as targets of tyrosine nitration, J. Clin. Investig. 108 (12) (2001) 1759–1770, https://doi.org/10.1172/JCI12617.
[62] S.W. Lee, H.K. Kim, P. Naidansuren, K.A. Ham, H.S. Choi, H.Y. Ahn, M. Kim, D. H. Kang, S.W. Kang, Y.A. Joe, Peroxidasin is essential for endothelial cell survival and growth signaling by sulfilimine crosslink-dependent matrix assembly, FASEB J. 34 (8) (2020) 10228–10241, https://doi.org/10.1096/fj.201902899R.
[63] T.A. Wynn, T.R. Ramalingam, Mechanisms of fibrosis: therapeutic translation for fibrotic disease, Nat. Med. 18 (7) (2012) 1028–1040, https://doi.org/10.1038/nm.2807.
[64] V.J. Thannickal, Y. Zhou, A. Gaggar, S.R. Duncan, Fibrosis: Ultimate and proximate causes, J. Clin. Investig. 124 (11) (2014) 4673–4677, https://doi.org/10.1172/JCI74368.